ANNALS OF GEOPHYSICS, 61,3, SE343, 2018; doi: 10.4401/ag-7649

“ANALYTICAL SEISMIC WAVE ATTENUATION AND VELOCITY DISPERSION IN LAYERED DOUBLE-POROSITY MEDIA”

Zhengyang Zhao[1,2], Xingyao Yin[1,2] and Zhaoyun Zong[1,2,*]

[(1)] China University of Petroleum, Qingdao, Shandong, China
[(2)] Laboratory for Marine Mineral Resources, Qingdao National Laboratory for Marine Science and Technology, Qingdao, Shandong, China

Article history
Receveid **February 4, 2017**; accepted **April 20, 2018.**
Subject classification:
Local fluid flow; Attenuation; Velocity dispersion; Layered double-porosity media; Wave equations.

ABSTRACT

Due to differences of rock properties such as porosity, permeability and compressibility between different regions in the porous media, pressure gradients are induced between those different regions and lead to local fluid flow. When seismic wave propagates in the porous media, the local fluid flow process is a main cause of wave attenuation and velocity dispersion. The local fluid flow mechanism of the layered porous model has been studied by many authors in the numerical approaches without analytical wave equations and solution for this kind of rock physics models. In this study, we first establish a layered double-porosity model saturated with a single fluid and derive the wave equations. According to the derived novel wave equations, then we calculate the phase velocity and quality factor in the layered double-porosity media based on plane wave analysis. The results demonstrate that there are three kinds of wave modes named as the fast P-wave and two slow P-wave in layered porous media when P-wave propagates through the model perpendicularly. Finally, we study the effects of local fluid flow on the mesoscopic loss mechanism by analyzing the attenuation and the velocity dispersion of seismic waves in the low frequency range.

1. INTRODUCTION

When seismic waves propagate in underground porous media saturated with fluid, pressure gradients are induced between different regions and lead to fluid flow relative to the solid. This kind of fluid flow is known as wave-induced fluid flow, which can lead to attenuation and velocity dispersion of seismic waves. According to the heterogeneities of the different scales, we can divide attenuation theories due to wave-induced fluid flow into macro-scale, micro-scale and meso-scale attenuation theory [Chapman et al., 2002; Müller et al., 2010].

Biot [1956, 1962] described quantitatively the wave attenuation and dispersion induced by macroscopic fluid flow. Mavko and Nur [1975, 1979] proposed a squirt-flow mechanism, which is a typical micro-scale attenuation theory. This theory emphasizes that because of the heterogeneity of the individual pore scale, the fluid in the pores is squeezed out the pores when seismic wave propagates in porous media. Squirt-flow mechanism predicts wave attenuation much higher than that predicted by Biot model. Dvorkin and Nur [1993] presented a uniform model named as BISQ model, which combined Biot theory and squirt-flow mechanism. This model, however, cannot describe seismic wave attenuation in the seismic frequency range.

White [1975] introduced a partially saturated porous model to describe the meso-scale attenuation and dispersion in the low frequency band. The meso-scale heterogeneity is much higher than individual pore scale and smaller than wavelength scale. Dutta and Odé [1979a, 1979b] analyzed the attenuation and velocity

dispersion for White model by solving the Biot's equations. Gurevich et al. [1997] considered a finely layered porous rock and calculated the P wave quality factor for this rock. Wang et al. [2013] studied the properties of wave attenuation and velocity dispersion with the variation of gas saturation and porosity based on the White model. Berryman and Wang [2000] developed phenomenological equations and obtained the coefficients in these equations to study oil and gas reservoirs contained storage porosity and fracture/crack porosity. Chen et al. [2016] thought that wave-induced fluid flow will be affected by the multi-phase fluid, and through the analyses of seismic wave attenuation and reflection behavior to verify. Pride et al. [2004] proposed a unified theory to analyze three P wave attenuation models for sedimentary rocks. The fluid flow due to heterogeneity is at different scales in each model. Sun et al. [2015] compared several analytical models to study the wave attenuation and dispersion due to wave-induced fluid flow and to analyze velocity-saturation relations. In order to study the P-wave dissipation process in a double-porosity media, Sun et al. [2016] proposed a triple-layer patchy model saturated with two immiscible fluids. Chapman et al. [2017] believed that the frequency scaling behavior of seismic attenuation is affected by the spatial distribution of the fluid, and they demonstrated this theory from the experimental investigation of the Berea sandstone saturated with two fluid phases.Local fluid flow (LFF) process induces wave attenuation and dispersion in the seismic frequency band when wave propagates in the porous media. To study the LFF process in the double-porosity medium, Ba et al. [2011] proposed a double-porosity model and derived the equations of motion for this model. However, the fluid kinetic energy inside the spherical pockets is neglected in this paper when they calculated the kinetic energy of the LFF process and the dissipation function. In order to solve this problem, Ba et al. [2014] derived the equations of motion by rewriting the kinetic energy function including the LFF velocities inside and outside the inclusions and the dissipation function. To predict the attenuation and dispersion in double-porosity media, Zheng et al. [2017] presented a new form of wave equations and solved these equations by using an analytical method. Ba et al. [2016] proposed a new double-porosity model to explain strong velocity dispersion in tight siltstone with clay-filled pores obtained from the experiment. To study the effects of fabric and saturation inhomogeneities on wave attenuation and velocity dispersion, Ba et al. [2017] proposed a double double-porosity model and derived the governing equations for this model based on Hamilton's principle. There are one fast P wave and four slow Biot waves in the media when the compressional waves propagate in the double double-porosity model. Based on the T matrix approach, Agersborg et al. [2009] modeled the effective viscoelastic properties of cracked porous media and explain the effects of LFF in double-porosity media. Song et al. [2016] proposed an analytical solution of effective dynamic shear modulus and analyzed the relation between wave-induced fluid flow and shear modulus by calculating the S wave attenuation and velocity dispersion. White et al. [1975] proposed a layered porous model which is saturated with both water and gas alternately. Pressure gradients between two layers induce LFF, namely, inter-layer flow which have been studied by many authors. Brajanovski et al. [2005] studied the influences of fractures on rock properties by modelling fractures as thin porous layers in porous media. Based on the propagator matrix approach, they obtained the effective P-wave modulus of the fractured porous material from the dispersion equation. Gelinsky et al. [1998] analyzed the effects of medium heterogeneity on P wave propagating in the layered medium and obtained the expressions of the phase velocity and the attenuation coefficient of P wave. Krzikalla and Müller [2011] performed elastic up-scaling of thinly layered rocks by using the established Backus averaging technique. Norris [1993] proposed a theory for the P wave attenuation and velocity dispersion in porous layered media saturated with fluid. In this work, we consider a layered double-porosity model to describe the wave-induced local fluid flow in porous layers, and analyze the mesoscopic loss mechanism due to LFF. In section 2, we first establish a layered double-porosity model containing two layers saturated with a single-fluid. Then we review the Hamilton's principle and derive the expressions of potential energy, kinetic energy and dissipation function including LFF term by extending the Biot-Rayleigh theory [Biot, 1956, 1962; Rayleigh, 1917; Ba et al., 2011]. Substituting the expressions of potential energy, kinetic energy and dissipation function into Lagrange's equations, we obtain the equations of motion for layered double-porosity model. In section 3, we perform the numerical simulations and analyze the effects of some rock parameters such as viscosity, permeability and thickness of layers on wave attenuation and velocity dispersion.

2. THEORY

2.1 LAYERED DOUBLE-POROSITY MODEL

Based on the White model, we first consider a layered double-porosity model containing two layers shown in Figure 1. Figure 1a shows a layered medium which contains of alternating layers saturated with two immiscible fluids. We choose an elementary volume in the laminated medium, as shown by the black box in the Figure 1a. Figure 1b is the diagram of the layered double-porosity model. It is interesting to note the layered double-porosity model and the elementary volume we choose are not exactly the same. Each layer in the layered double-porosity model has a different porosity but is saturated with the same fluid. Assume that ϕ_{10} and ϕ_{20} are the porosity in upper and lower layers, respectively. The absolute porosities of two layers can be written as $\phi_m = V_m \phi_{m0}$, $m = 1, 2$, where V_m, $m = 1, 2$ are the volume fraction of upper and lower layers relative to the model, respectively. The total porosity of the model is $\phi = \phi_1 + \phi_2$. Moreover, we denote the thickness of upper layer by X_1 and the total thickness of the model by X_2, the length and the width of the model by l_1 and l_2, respectively.

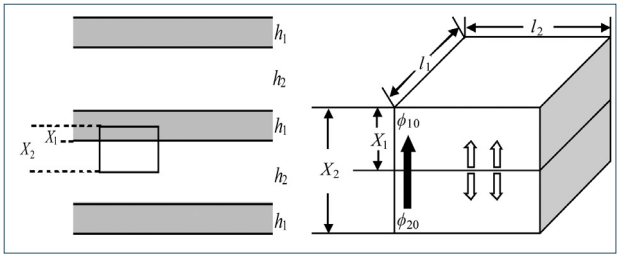

FIGURE 1. A diagram of layered model: (a) layered White model; (b) layered double-porosity model.

To analyze the propagation mechanism of the seismic waves, we consider the following assumptions: (1) each layer in the layered double-porosity model is isotropic and homogeneous; (2) there is no fluid flow across the top and the bottom of the model and the boundary conditions between the two layers are open; (3) the wavelength of the seismic wave is much longer than the total thickness of the model. Macro-flow and LFF are induced when P wave propagates through model perpendicularly, as shown by black arrow and white arrow in Figure 1, respectively. We denote the dynamic thickness of fluid in upper layer by X, which is a function of time.

We denote by x_i, i = 1, 2, 3 the spatial variables and by t the time variable, the displacement vector of the solid by u_i and the average fluid displacement vector in two layers by $U_i^{(m)}$, $m = 1, 2$, respectively. Furthermore, we define the strain components of the displacement vector of the solid and fluid:

$$e_{ij} = \frac{1}{2}\left(\frac{\partial u_i}{\partial x_j} + \frac{\partial u_j}{\partial x_i}\right) \text{ and } \xi_{ij}^{(m)} = \frac{1}{2}\left(\frac{\partial U_i^{(m)}}{\partial x_j} + \frac{\partial U_j^{(m)}}{\partial x_i}\right) \tag{1}$$

and introduce the bulk strain of the solid and fluid as

$$e = e_{ii} = \frac{\partial u_1}{\partial x_1} + \frac{\partial u_2}{\partial x_2} + \frac{\partial u_3}{\partial x_3} \text{ and}$$
$$\xi_m = \xi_{ii}^{(m)} = \frac{\partial U_1^{(m)}}{\partial x_1} + \frac{\partial U_2^{(m)}}{\partial x_2} + \frac{\partial U_3^{(m)}}{\partial x_3} \tag{2}$$

2.2 HAMILTON'S PRINCIPLE

In order to study the attenuation and velocity dispersion of seismic waves in layered porous media, we derive the equations of motion by using the Hamilton's principle. The Lagrange energy density can be expressed as

$$L = T - W \tag{3}$$

where T and W are the kinetic energy and potential energy in the model, respectively. The Lagrange's equations can be written as

$$\partial_t\left(\frac{\partial L}{\partial \dot{u}_i}\right) + \partial_j\left[\frac{\partial L}{\partial\left(\partial_j u_i\right)}\right] + \frac{\partial D}{\partial \dot{u}_i} = 0 \tag{4}$$

where u_i is the generalized coordinates, denoting the displacement vectors u_i, $U_i^{(1)}$ and $U_i^{(2)}$, respectively; D is the dissipation function. The point above a variable represents the derivative of the time. The governing equation can be expressed as

$$\partial_t\left(\frac{\partial L}{\partial \dot{\delta}}\right) + \frac{\partial L}{\partial \delta} + \frac{\partial D}{\partial \dot{\delta}} = 0 \tag{5}$$

where the δ is the bulk strain increment of fluid due to LFF. In order to obtain the equations of motion for layered double-porosity model, we need to derive the expressions of potential energy, kinetic energy and dissipation function and substitute these expressions into Lagrange's equations and governing equation.

2.3 EXPRESSION OF POTENTIAL ENERGY FUNCTION

The potential energy function of layered double-porosity media has five independent variables, which can be expressed as

$$W = W\left(I_1, I_2, I_3, \xi_1, \xi_2\right) \tag{6}$$

where I_1, I_2 and I_1 are the first, second and third invariants of solid strain; ξ_1 and ξ_2 denote the fluid volumetric strain in upper and lower layers, respectively. Based on Ba et al., [2011], the strain energy function in the layered double-porosity media can be written as:

$$2W = \left(A+2N\right)I_1^2 - 4NI_2 + 2Q_1 I_1\left(\xi_1 - \phi_2\delta\right) + R_1\left(\xi_1 - \phi_2\delta\right)^2 + 2Q_2 I_1\left(\xi_2 + \phi_1\delta\right) + R_2\left(\xi_2 + \phi_1\delta\right)^2, \quad (7)$$

where A, N, Q_1, Q_2, R_1, R_2 are the six elastic coefficients (see Appendix A). Here we used Taylor expansion and ignored the higher order terms beyond the second order in the derivation. According to the mass conservation of fluid, we can get $\phi_1(-\phi_2\delta) + \phi_2(\phi_1\delta) = 0$.

The effective variation of fluid volume in upper layer is $\phi_2\delta \approx 1 - V_1/V$, where V_1 and V are the fluid static and dynamic volume in upper layer whose the thicknesses are X_1 and X, respectively. Then, the bulk strain increment of fluid δ can be expressed as:

$$\delta = \frac{1}{\phi_2}\left(1 - \frac{X_1}{X}\right) \quad (8)$$

2.4 EXPRESSIONS OF KINETIC ENERGY AND DISSIPATION FUNCTION

The kinetic energy function for layered double-porosity model can be written as:

$$2T = \rho_0 \sum_i \dot{u}_i^2 + \rho_f \sum_m \int_{V_{\phi_m}} \sum_i \left(\dot{u}_i + v_{global,i}^{(m)} + v_{local,i}^{(m)}\right)^2 dV_{\phi_m} \quad (9)$$

where

$$\rho_0 = (1 - \phi)\,\rho_s \quad (10)$$

with ρ_s and ρ_f denoting the solid and fluid mass densities, respectively; $v_{global,i}^{(m)}$ and $v_{local,i}^{(m)}$ denote relative velocity of the global flow and inter-layer local flow of fluid in two layers, respectively; $V_{\phi m}$ is the pore volume. $\sum_i$ and $\sum_m$ are the summation symbols, which denote summation corresponding to the Cartesian coordinates and summation corresponding to the two layers, respectively.

Expanding the second item on the right of the Equation (9) gives

$$\begin{aligned}&\rho_f \sum_m \int_{V_{\phi_m}} \sum_i \left(\dot{u}_i + v_{global,i}^{(m)} + v_{local,i}^{(m)}\right)^2 dV_{\phi_m} \\ &= \rho_f \sum_m \int_{V_{\phi_m}} \sum_i [\dot{u}_i^2 + (v_{global,i}^{(m)})^2 + (v_{local,i}^{(m)})^2 + 2\dot{u}_i v_{global,i}^{(m)} \\ &\quad + 2\dot{u}_i v_{local,i}^{(m)} + 2v_{global,i}^{(m)} v_{local,i}^{(m)}]dV_{\phi_m}.\end{aligned} \quad (11)$$

Let us analyze the terms

$$2\rho_f \sum_m \int_{V_{\phi_m}} \sum_i \left(\dot{u}_i v_{local,i}^{(m)} + v_{global,i}^{(m)} v_{local,i}^{(m)}\right) dV_{\phi_m} \quad (12)$$

The relative velocity of the global fluid flow $v_{global,i}^{(m)}$ can be expressed as

$$v_{global,i}^{(m)} = \dot{U}_i^{(m)} - \dot{u}_i \quad (13)$$

Substituting the Equation (13) into Equation (12) gives

$$\begin{aligned}&2\rho_f \sum_m \int_{V_{\phi_m}} \sum_i \left(\dot{u}_i v_{local,i}^{(m)} + v_{global,i}^{(m)} v_{local,i}^{(m)}\right) dV_{\phi_m} \\ &= 2\rho_f \sum_m \int_{V_{\phi_m}} \sum_i \dot{U}_i^{(m)} v_{local,i}^{(m)}\, dV_{\phi_m}\end{aligned} \quad (14)$$

Assume that the angle between the propagating direction of the P wave and the normal direction of the interface between two layers is θ, we have $v_{local,i}^{(m)} = \cos\theta \dot{U}_i^{(m)}$. Since the propagating direction of the P wave is perpendicular to the interface between two layers, the velocity of inter-layer flow and the absolute velocity of fluid flow are equal, which can be written as $v_{local,i}^{(m)} = \dot{U}_i^{(m)}$. Substituting this formula into Equation (14), we have

$$\begin{aligned}&2\rho_f \sum_m \int_{V_{\phi_m}} \sum_i \left(\dot{u}_i v_{local,i}^{(m)} + v_{global,i}^{(m)} v_{local,i}^{(m)}\right) dV_{\phi_m} \\ &= 2\rho_f \sum_m \int_{V_{\phi_m}} \sum_i \left(v_{local,i}^{(m)}\right)^2 dV_{\phi_m}.\end{aligned} \quad (15)$$

Substituting the Equations (11), (13) and (15) into Equation (9) gives

$$2T = \rho_{00} \sum_i \dot{u}_i^2 + 2\sum_m \rho_{0m} \sum_i \dot{u}_i \dot{U}_i^{(m)} + \sum_m \rho_{mm} \sum_i \left(\dot{U}_i^{(m)}\right)^2 + 2T_L \quad (16)$$

where

$$2T_L = 3\rho_f \sum_m \int_{V_{\phi_m}} \sum_i \left(v_{local,i}^{(m)}\right)^2 dV_{\phi_m} \quad (17)$$

is the kinetic energy function of the LFF process and ρ_{00}, ρ_{0m}, ρ_{mm} are five density coefficients (see Appendix A).

The dissipation function in this case is

$$2D = \sum_m b_m \sum_i \left(\dot{U}_i^{(m)} - \dot{u}_i\right)^2 + 2D_L \quad (18)$$

where

$$b_m = V_m' \phi_{m0}^2 \left(\frac{\eta}{\kappa_m}\right) = \phi_m \phi_{m0} \left(\frac{\eta}{\kappa_m}\right) \quad (19)$$

denote the dissipative coefficients in upper and lower layers; η and κ_m denote the viscosity and the permeability of upper and lower layers, respectively; D_L is the dissipation function of the LFF process.

2.5 KINETIC ENERGY AND DISSIPATION FUNCTION OF THE LFF PROCESS

In this section, we derive the expression of the kinetic energy and dissipation function of the LFF process by using the generalization of Rayleigh's theory. First, we calculate the fluid velocity in upper and lower layers, respectively. The one-dimensional continuity equation of fluid in upper layer is

$$\frac{d\rho_f}{dt}+\rho_f\frac{\partial \dot{x}_{upper}}{\partial x}=0 \tag{20}$$

where $\dot{x}_{upper}$ denote the fluid particle velocity in upper layer. After the calculation of the Equation (20), we have

$$\dot{x}_{upper}=\frac{\dot{X}}{X}x \tag{21}$$

where $\dot{X}$ denote the fluid particle velocity at the interface between two layers. Generalizing Rayleigh's theory to the layered double-porosity model, we have

$$\phi_{10}\dot{X}=\phi_{20}\dot{x}_{lower} \tag{22}$$

where $\dot{x}_{lower}$ denote the fluid particle velocity in lower layer.

Second, we derive the kinetic energy function of the LFF process in upper and lower layers, respectively. The kinetic energy function of the LFF process in upper layer is

$$T_{upper}=\frac{3}{2}\rho_f\phi_{10}\int_0^X l_1l_2\dot{x}_{upper}^2\,dx=\frac{1}{2}\rho_f\phi_{10}l_1l_2\dot{X}^2X \tag{23}$$

The fluid kinetic energy of the LFF process in lower layer is

$$T_{lower}=\frac{3}{2}\rho_f\phi_{20}\int_X^{X_2} l_1l_2\dot{x}_{lower}^2\,dx=\frac{3}{2}\rho_f\frac{\phi_{10}^2}{\phi_{20}}l_1l_2\dot{X}^2\left(X_2-X\right) \tag{24}$$

Thus the kinetic energy of the LFF process can be described as the sum of the fluid kinetic energy of upper and lower layers, i.e.

$$T_L=T_{upper}+T_{lower}=\frac{1}{2}\rho_f\phi_{10}l_1l_2\dot{X}^2X+\frac{3}{2}\rho_f\frac{\phi_{10}^2}{\phi_{20}}l_1l_2\dot{X}^2\left(X_2-X\right) \tag{25}$$

The volume fraction of upper layer is $V_1=l_1l_2X_1\approx l_1l_2X_1$. Using this equation and $\phi_1=V_1\,\phi_{10}$, we have

$$X=\frac{\phi_1}{l_1l_2\phi_{10}} \tag{26}$$

From Equation (8) we have

$$\dot{X}=X_1\phi_2\dot{\delta} \tag{27}$$

Substituting the Equations (26) - (27) into Equation (25) gives

$$T_L=\frac{1}{2}\rho_f\phi_1\phi_2^2X_1^2\dot{\delta}^2+\frac{3}{2}\rho_f\frac{\phi_{10}^2\phi_2^2}{\phi_{20}}l_1l_2X_1^2\left(X_2-\frac{\phi_1}{l_1l_2\phi_{10}}\right)\dot{\delta}^2 \tag{28}$$

Similarly, the dissipation function of the LFF process can be written as

$$D_L=\frac{1}{2}\phi_{10}^2\left(\frac{\eta}{\kappa_1}\right)\int_0^X l_1l_2\dot{x}_{upper}^2\,dx+\frac{1}{2}\phi_{20}^2\left(\frac{\eta}{\kappa_2}\right)\int_X^{X_2} l_1l_2\dot{x}_{lower}^2\,dx \tag{29}$$

Using Equations (21), (22), (26) and (27), we obtain

$$D_L=\frac{1}{6}\left(\frac{\eta}{\kappa_1}\right)\phi_1\phi_{10}\phi_2^2X_1^2\dot{\delta}^2+\frac{1}{2}\left(\frac{\eta}{\kappa_2}\right)\phi_{10}^2\phi_2^2l_1l_2X_1^2\left(X_2-\frac{\phi_1}{l_1l_2\phi_{10}}\right)\dot{\delta}^2 \tag{30}$$

2.6 EQUATIONS OF MOTION AND PLANE WAVE ANALYSIS

Substituting the expressions of potential energy, kinetic energy and dissipation function into Equations (4) and (5), and assuming the seismic wave propagates along the x_1 direction, we derive the following equations of motion:

$$\begin{aligned}&N\nabla^2u_1+\left(A+N\right)\frac{\partial e}{\partial x_1}+Q_1\frac{\partial}{\partial x_1}\left(\xi_1-\phi_2\delta\right)+Q_2\frac{\partial}{\partial x_1}\left(\xi_2+\phi_1\delta\right)\\&=\rho_{00}\ddot{u}_1+\rho_{01}\ddot{U}_1^{(1)}+\rho_{02}\ddot{U}_1^{(2)}+b_1\left(\dot{u}_1-\dot{U}_1^{(1)}\right)+b_2\left(\dot{u}_1-\dot{U}_1^{(2)}\right),\end{aligned} \tag{31a}$$

$$Q_1\frac{\partial e}{\partial x_1}+R_1\frac{\partial}{\partial x_1}\left(\xi_1-\phi_2\delta\right)=\rho_{01}\ddot{u}_1+\rho_{11}\ddot{U}_1^{(1)}-b_1\left(\dot{u}_1-\dot{U}_1^{(1)}\right) \tag{31b}$$

$$Q_2\frac{\partial e}{\partial x_1}+R_2\frac{\partial}{\partial x_1}\left(\xi_2+\phi_1\delta\right)=\rho_{02}\ddot{u}_1+\rho_{22}\ddot{U}_1^{(2)}-b_2\left(\dot{u}_1-\dot{U}_1^{(2)}\right) \tag{31c}$$

$$\begin{aligned}&\phi_1Q_2e+\phi_1R_2\left(\xi_2+\phi_1\delta\right)-\phi_2Q_1e-\phi_2R_1\left(\xi_1-\phi_2\delta\right)\\&=\rho_f\phi_2^2X_1^2\left[\phi_1+3\frac{\phi_{10}^2}{\phi_{20}}l_1l_2\left(X_2-\frac{\phi_1}{l_1l_2\phi_{10}}\right)\right]\ddot{\delta}\\&+\phi_{10}\phi_2^2X_1^2\left[\frac{1}{3}\frac{\eta}{\kappa_1}\phi_1+\frac{\eta}{\kappa_2}\phi_{10}l_1l_2\left(X_2-\frac{\phi_1}{l_1l_2\phi_{10}}\right)\right]\dot{\delta}\end{aligned} \tag{31d}$$

We indicate the unknowns of Equations (31a) ~ (31d) as the form of plane wave solutions

$$\begin{aligned}&u_1=u_{10}e^{i\left(\omega t-k_1\cdot x_1\right)},\ U_1^{(1)}=U_{10}^{(1)}e^{i\left(\omega t-k_1\cdot x_1\right)},\\&U_1^{(2)}=U_{10}^{(2)}e^{i\left(\omega t-k_1\cdot x_1\right)},\ \delta=\delta_0e^{i\left(\omega t-k_1\cdot x_1\right)},\end{aligned} \tag{32}$$

where ω denote the angular frequency, and $k_1=k_{10}-i\alpha$ is the complex wave number, with k_{10} and α denoting the real wave number and attenuation coefficient. Substituting Equation (32) into Equation (31d) gives the expression of δ. Then substituting the expression of δ and Equation (32) into Equations (31a) ~ (31c) gives three solutions of P wave number (see Appendix B).

The complex velocity and the phase velocity can be expressed as

$$\tilde{v}=\frac{\omega}{k_1}\ \text{and}\ v=\left[\mathrm{Re}\left(\frac{1}{\tilde{v}}\right)\right]^{-1} \tag{33}$$

and the attenuation factor and the quality factor can be written as

$$\alpha = -\omega \operatorname{Im}\left(\frac{1}{\tilde{v}}\right) \text{ and } Q = \frac{\pi f}{\alpha v} = \frac{\operatorname{Re}\left(\tilde{v}\right)}{2\operatorname{Im}\left(\tilde{v}\right)} \tag{34}$$

where f = ω/2π is frequency.

3. NUMERICAL SIMULATIONS

In order to verify the correctness of the method in this work, we calculate the phase velocities and quality factors of the three P waves respectively, and compare these results with those of White et al. (1975). The rock parameters involved in the calculation process are shown in Table 1, where K_s, μ_s and ρ_s are the bulk modulus, shear modulus and mass density of solid grains; K_f and ρ_f are the bulk modulus and mass density of the pore fluid; c_1 and c_2 are the consolidation parameters of upper and lower layers, and c_s are the shear consolidation parameter.

Parameter	Value	Parameter	Value
K_s (GPa)	38	l_1 (m)	0.2
μ_s (GPa)	44	l_2 (m)	0.2
ρ_s (kg/m3)	2650	κ_1 (D)	1
K_f (GPa)	2.5	κ_2 (D)	0.01
ρ_f (kg/m3)	1040	ϕ_{10}	0.3
η (Pa s) (ambient water)	0.001	ϕ_{20}	0.1
η (Pa s) (oil)	0.005	c_1	200
η (Pa s) (hot water)	0.0002	c_2	10
X_2 (m)	0.2	c_s	10

TABLE 1. Rock parameters of layered double-porosity media.

The dry rock bulk moduli of upper and lower layers can be expressed as

$$K_{bm} = \frac{\left(1-\phi_{m0}\right)K_s}{1+c_m\phi_{m0}} \tag{35}$$

the dry rock bulk modulus of the model can be written as

$$\frac{1}{K_b} = \frac{V_1'}{K_{b1}} + \frac{V_2'}{K_{b2}} \tag{36}$$

and the dry rock shear modulus of the model can be expressed as

$$\mu_b = \frac{\left(1-\phi\right)\mu_s}{1+c_s\phi} \tag{37}$$

Figure 2 shows the phase velocity (Figure 2a) and the dissipation factor (Figure 2b) of the fast P wave for different fluids, where the thickness of upper layer X_1 = 0.1 m. As is shown in Figure 2a, the phase velocities increase with frequency in the low frequency range. LFF process induces the velocity dispersion. Moreover, the curves of phase velocity move toward low frequencies with increasing of the fluid viscosity. As is shown in Figure 2b, the curves of dissipation factor have two peaks, one of which induced by LFF process is in the low frequency band, the other caused by Biot's friction is in the high frequency band. In addition, the low frequency peaks move toward the low frequencies with the increase of the fluid viscosity. The black solid lines in Figure 2 are the results calculated by White et al. [1975]. As is shown in Figure 2, the two results predicted by the layered double-porosity model and the layered White model are similar in the low frequency band, which can verify the correctness of the method in this work (Since the layered White model focuses on the attenuation and velocity dispersion of seismic waves in the low frequency range, the black solid lines have no attenuation peak and dispersion in the high frequency range).

Then we analyze the effects of the thickness of upper layer on the phase velocity and the dissipation factor. Here we use two ways to change the thickness of upper layer: (1) only the thickness of upper layer is changed and the thickness of the model is a constant; (2) the thicknesses of upper layer and the model are changed

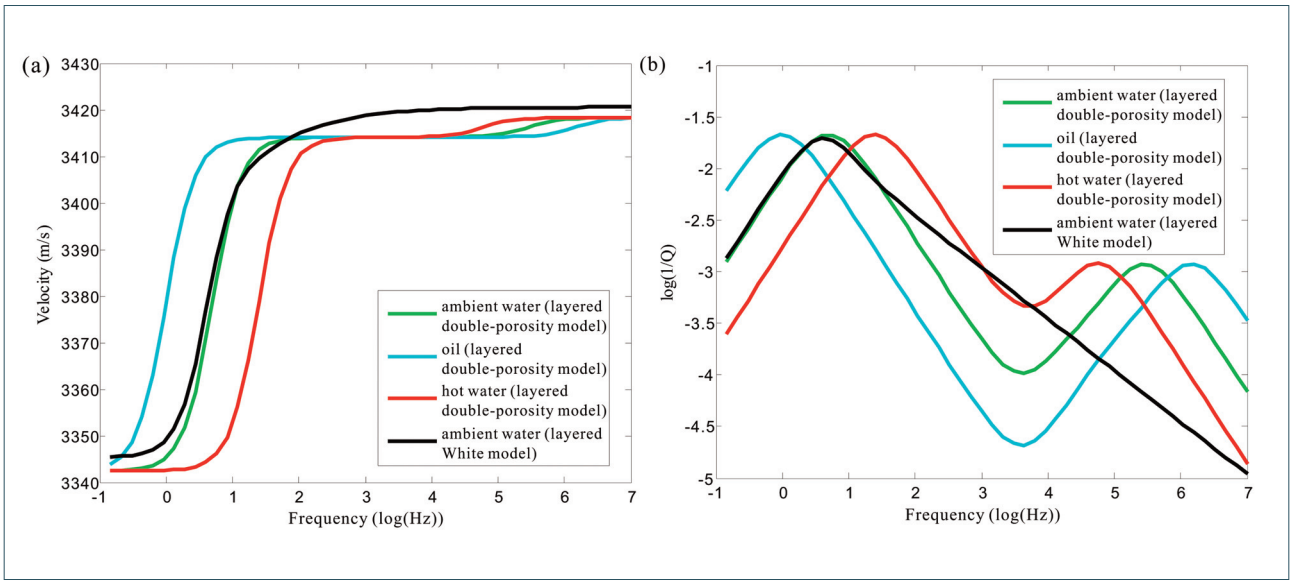

FIGURE 2. P wave (a) phase velocity and (b) dissipation factor for different fluids.

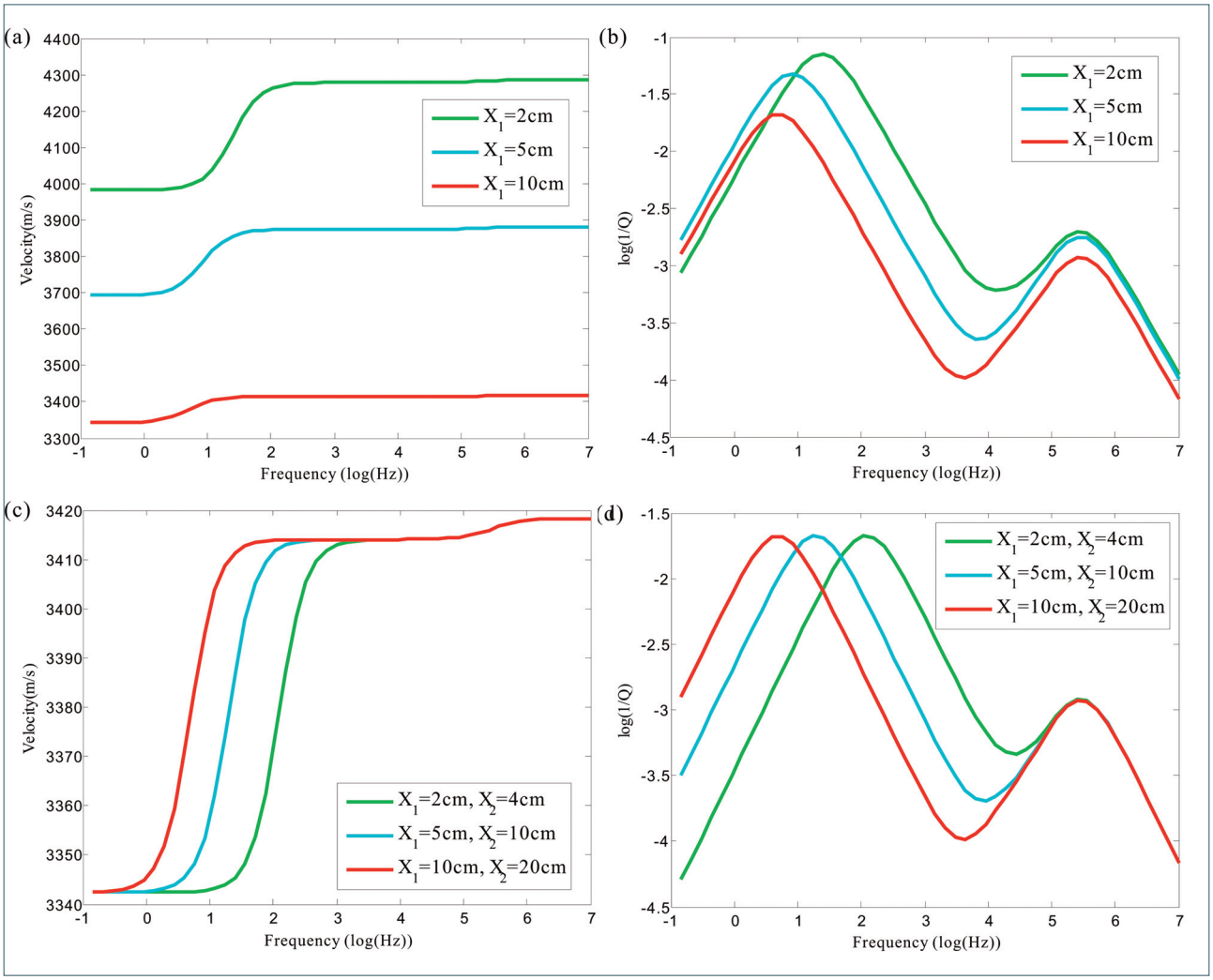

FIGURE 3. P wave (a), (c) phase velocity and (b), (d) dissipation factor for different thicknesses of upper layer.

simultaneously to ensure they satisfied $X_2 = 2X_1$.

Figure 3 displays the phase velocity (Figure 3a) and the dissipation factor (Figure 3b) of the fast P wave obtained using the first way, where the model saturates

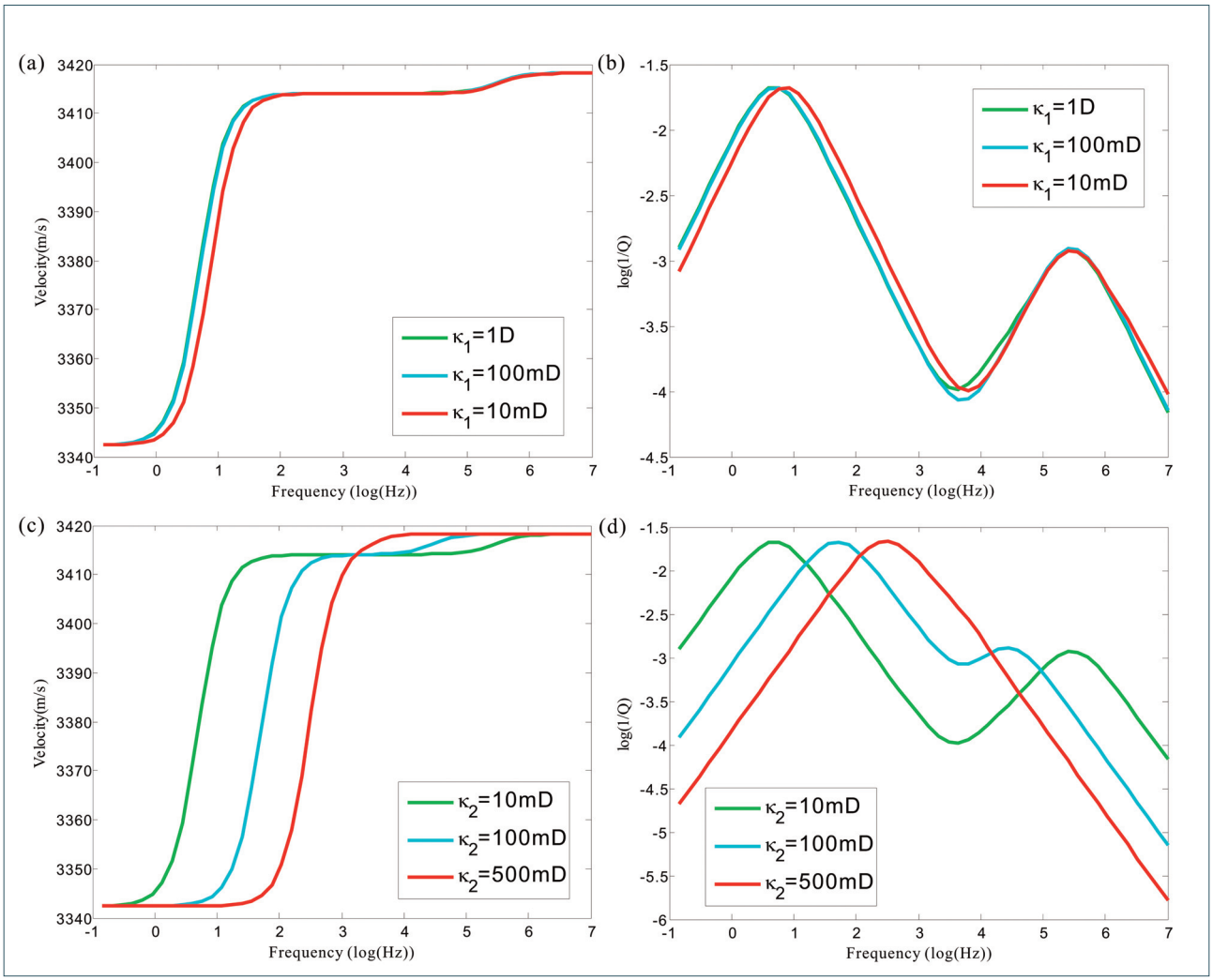

FIGURE 4. P wave (a), (c) phase velocity and (b), (d) dissipation factor for different permeability.

the ambient water. The velocity dispersion and the attenuation become obvious with decreasing of the thickness of upper layer or increasing of the thickness of lower layer, which illustrate high-porosity high-permeability thin layer can induce high velocity dispersion and strong attenuation. The results obtained by using the second way are shown in Figure 3c and 3d. The curves of phase velocity in the low frequency band and the LFF peaks move toward low frequencies with the increase of the thickness of upper layer.

Figure 4 displays the phase velocity (Figure 4a and 4c) and the dissipation factor (Figure 4b and 4d) of the fast P wave for different permeability, where the thickness of upper layer X_1 = 0.1 m and the model saturates the ambient water. As is shown in Figure 4, the curves of phase velocity and dissipation factor do not change significantly with decreasing of the permeability of the upper layer. Furthermore, the curves of phase velocity and the LFF peaks move toward high frequencies with the increase of the permeability of the lower layer. These results indicate that the effective permeability of the model should be determined by the layer with lower permeability when the permeability of two layers is different. Therefore the effective permeability of the model does not change very much when the permeability of the layer with higher permeability changes, so that the influence on attenuation and velocity dispersion is not significant. However, the effective permeability of the model will increase with the increase of permeability of the layer with lower permeability, which leads to the curves of phase velocity and the LFF peaks move toward high frequencies.

In this study, we obtain two slow P waves (P2 and P3), whose phase velocity and dissipation factor for different fluids are shown in Figure 5. Figure 6 displays the phase velocity (Figure 6a and 6c) and the dissipation factor (Figure 6b and 6d) of two slow P waves by using the two ways of changing thickness. In the low frequency range, the P2 and P3 waves are dominated by the diffusive mode, and the internal friction between

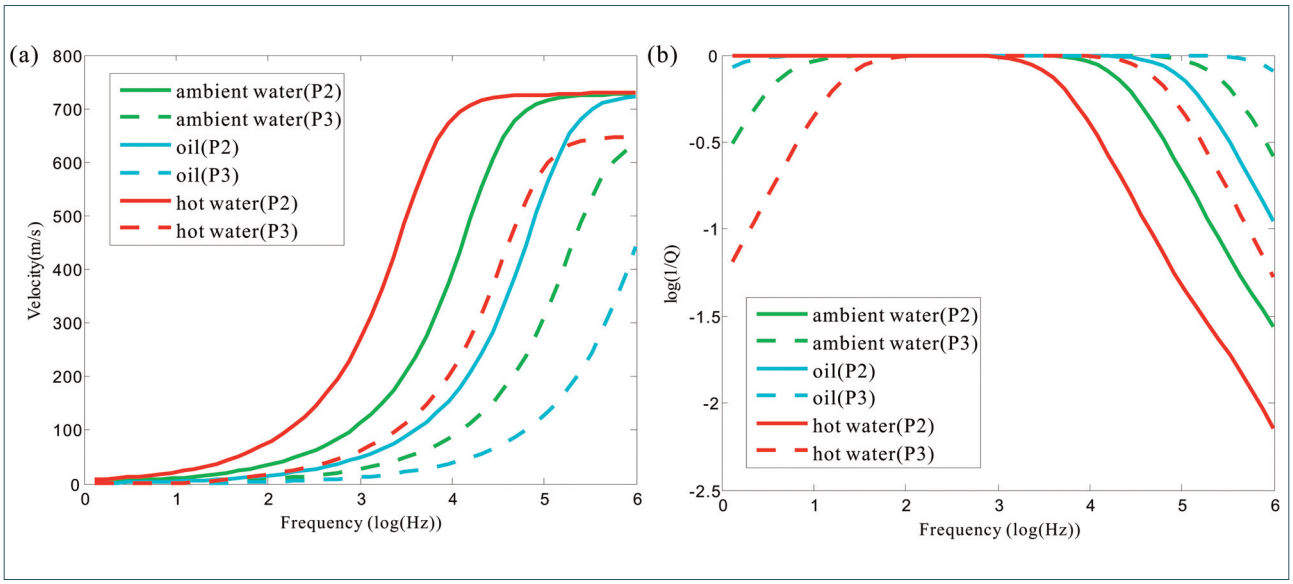

FIGURE 5. P2 and P3 wave (a) phase velocities and (b) dissipation factors for different fluids.

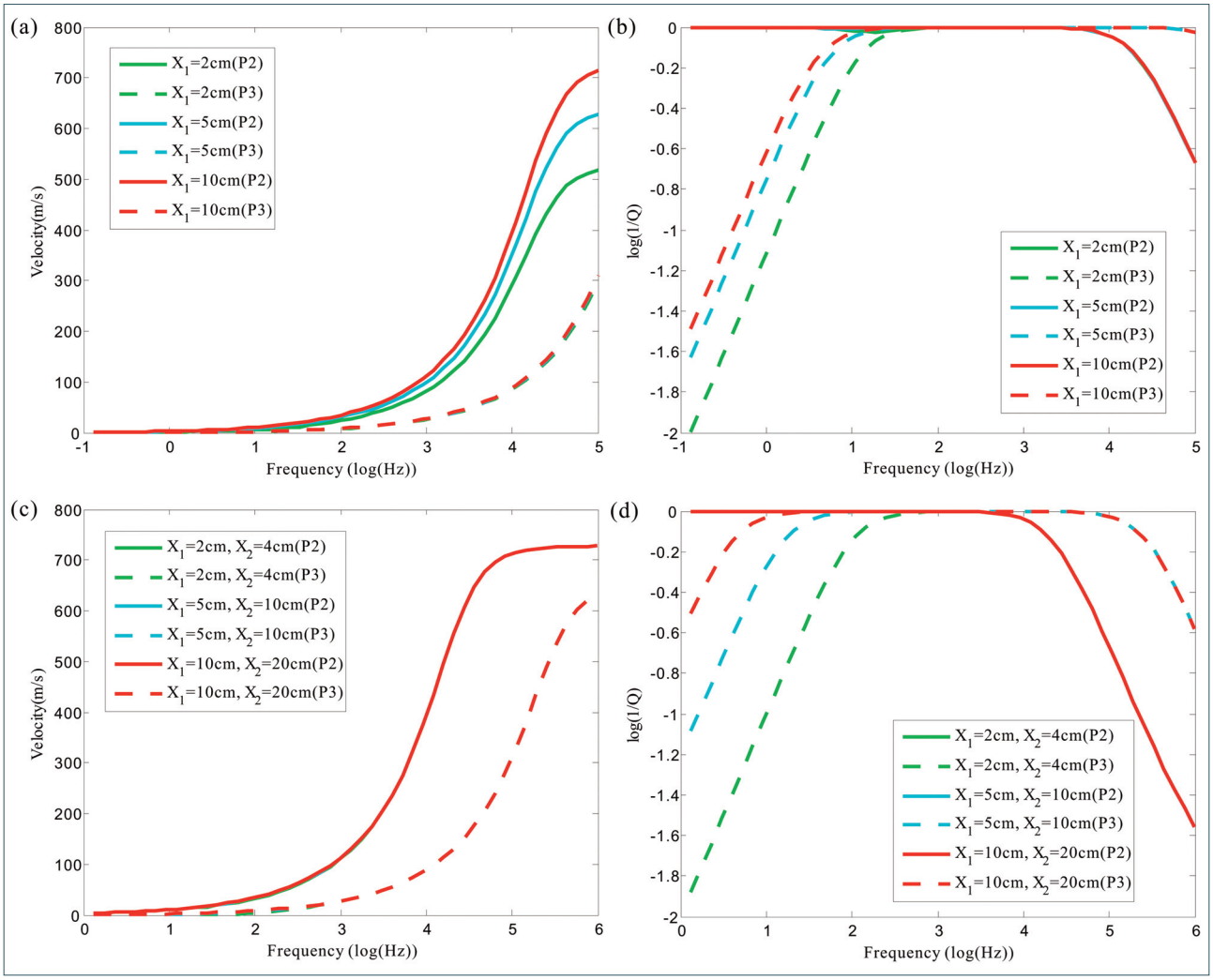

FIGURE 6. P2 and P3 wave (a), (c) phase velocities and (b), (d) dissipation factors for different thicknesses of upper layer.

the solid and the fluid is the main cause of their attenuation and dispersion. The phase velocities of P2 and P3 waves close to zero at low frequencies, and increase with frequency. The dissipation factor of P2 wave close

to zero at low frequencies, and decrease with frequency. In addition, the dissipation factor of P3 wave increase with frequency in the low frequency range and decrease with frequency in the high frequency band.

4. CONCLUSIONS

We presented a layered double-porosity model and derived the equations of motion to study the effects of rock properties on seismic wave attenuation and velocity dispersion in isotropic poro-elastic media. Based on the White model, the present model consists of two layers saturated with a single-fluid. According to the Hamilton's principle and the extension of Biot-Rayleigh theory, we derived the equations of motion by calculating the expressions of potential energy, kinetic energy and dissipation function and obtained three P wave modes. In the numerical simulation, we calculated the phase velocity and quality factor for these three P waves. The fast P wave attenuation and velocity dispersion are induced by LFF process in the low frequency range. The curves of phase velocity and the low frequency peaks move toward seismic frequency band with the increase of viscosity or the decrease of permeability. The internal friction force leads to the attenuation and velocity dispersion of two slow P waves. This study fully indicates that local fluid flow is a main cause of the mesoscopic loss mechanism in the layered double-porosity medium. However, this study doesn't consider the patchy saturation and the situation of oblique incident of seismic wave. These questions will be analyzed in a future work.

Acknowledgements. We would like to acknowledge the sponsorship of National Nature Science Foundation of China (U1762103, U1562215), National Grand Project for Science and Technology (2016ZX05024004; 2017ZX05009001; 2017ZX05036005; 2017ZX05032003), Science Foundation from SINOPEC Key Laboratory of Geophysics and Young Elite Scientists Sponsorship Program by CAST (2017QNRC001).

Appendix A: Expressions of Elastic and Density coefficients

According to Ba et al., [2011], the expressions of elastic coefficients are

$$A=\left(1-\phi\right)K_s-\frac{2}{3}N-\frac{K_s}{K_f}\left(Q_1+Q_2\right),\ N=\mu_b,$$
$$Q_1=\frac{\beta\phi_1K_s}{\beta+\gamma},\ Q_2=\frac{\phi_2K_s}{1+\gamma},\ R_1=\frac{\phi_1K_f}{\beta/\gamma+1},\ R_2=\frac{\phi_2K_f}{1/\gamma+1}, \tag{A1}$$

Where

$$\beta=\frac{\phi_{20}\left[1-\left(1-\phi_{10}\right)\frac{K_s}{K_{b1}}\right]}{\phi_{10}\left[1-\left(1-\phi_{20}\right)\frac{K_s}{K_{b2}}\right]}\ \text{and}\ \gamma=\frac{K_s\left(\beta\phi_1+\phi_2\right)}{K_f\left(1-\phi-\frac{K_b}{K_s}\right)} \tag{A2}$$

The expressions of density coefficients are

$$\rho_{00}=\left(1-\phi\right)\rho_s-\frac{1}{2}\left(\phi-1\right)\rho_f,$$
$$\rho_{01}=\frac{1}{2}\left(\phi_1-V_1^{'}\right)\rho_f,\ \rho_{02}=\frac{1}{2}\left(\phi_2-V_2^{'}\right)\rho_f, \tag{A3}$$
$$\rho_{11}=\frac{1}{2}\left(\phi_1+V_1^{'}\right)\rho_f,\ \rho_{22}=\frac{1}{2}\left(\phi_2+V_2^{'}\right)\rho_f$$

Appendix B: Solutions of P Wave Number

Substituting the Equation (32) into Equations (31a) ~ (31c), we obtain the equation for P wave number:

$$\begin{pmatrix} a_{11}k^2+b_{11} & a_{12}k^2+b_{12} & a_{13}k^2+b_{13} \\ a_{21}k^2+b_{21} & a_{22}k^2+b_{22} & a_{23}k^2+b_{23} \\ a_{31}k^2+b_{31} & a_{32}k^2+b_{32} & a_{33}k^2+b_{33} \end{pmatrix}\begin{pmatrix} u_{10} \\ U_{10}^{(1)} \\ U_{10}^{(2)} \end{pmatrix}=0 \tag{B1}$$

where

$$\begin{aligned}
&a_{11}=P+p_1^2/S, && a_{12}=Q_1-p_1p_2/S, && a_{13}=Q_2+p_1p_3/S,\\
&a_{21}=a_{12}, && a_{22}=R_1+p_2^2/S, && a_{23}=-p_2p_3/S,\\
&a_{31}=a_{13}, && a_{32}=a_{23}, && a_{33}=R_2+p_3^2/S,\\
&b_{11}=-\rho_{00}\omega^2+\mathrm{i}\omega\left(b_1+b_2\right), && b_{12}=-\rho_{01}\omega^2-\mathrm{i}\omega b_1, && b_{13}=-\rho_{02}\omega^2-\mathrm{i}\omega b_2,\\
&b_{21}=b_{12}, && b_{22}=-\rho_{11}\omega^2+\mathrm{i}\omega b_1, && b_{23}=0,\\
&b_{31}=b_{13}, && b_{32}=b_{23}, && b_{33}=-\rho_{22}\omega^2+\mathrm{i}\omega b_2,
\end{aligned} \tag{B2}$$

$$P=A+2N,$$
$$S=\left(\mathrm{i}\omega\right)\phi_{10}\phi_2^2X_1^2\left[\frac{1}{3}\frac{\eta}{\kappa_1}\phi_1+\frac{\eta}{\kappa_2}\phi_{10}l_1l_2\left(X_2-\frac{\phi_1}{l_1l_2\phi_{10}}\right)\right]$$
$$-\omega^2\rho_f\phi_2^2X_1^2\left[\phi_1+3\frac{\phi_{10}^2}{\phi_{20}}l_1l_2\left(X_2-\frac{\phi_1}{l_1l_2\phi_{10}}\right)\right]-\left(\phi_1^2R_2+\phi_2^2R_1\right),$$
$$p_1=\phi_1Q_2-\phi_2Q_1,\quad p_2=\phi_2R_1,\quad p_3=\phi_1R_2. \tag{B3}$$

REFERENCES

Agersborg, R., Johansen, T. A. and Jakobsen, M. (2009). Velocity variations in carbonate rocks due to dual porosity and wave-induced fluid flow, Geophysical Prospecting, 57(1), 81-98.

Ba, J., Carcione, J. M. and Nie, J. X. (2011). Biot-Rayleigh

theory of wave propagation in double-porosity media, Journal of Geophysical Research Atmospheres, 116(B06202), 1-12.

Ba, J., Zhang, L. and Sun, W. T. (2014). Velocity field of wave-induced local fluid flow in double-porosity media, Science China Physics, Mechanics & Astronomy, 57(6), 1020-1030.

Ba, J., Zhao, J. and Carcione, J. M. (2016). Compressional wave dispersion due to rock matrix stiffening by clay squirt flow, Geophysical Research Letters, 43(12), 6186-6195.

Ba, J., Xu, W. H. and Fu, L. Y. (2017). Rock anelasticity due to patchy saturation and fabric heterogeneity: A double double-porosity model of wave propagation, Journal of Geophysical Research: Solid Earth, 122(3), 1949-1976.

Berryman, J. G. and Wang, H. F. (2000). Elastic wave propagation and attenuation in a double-porosity dual-permeability medium, International Journal of Rock Mechanics and Mining Sciences, 37(1-2), 63-78.

Biot, M. A. (1956). Theory of propagation of elastic waves in fluid-saturated porous solid. I. Low-frequency range, Journal of the Acoustical Society of America, 28(2), 168-178.

Biot, M. A. (1962). Mechanics of deformation and acoustic propagation in porous media, Journal of Applied Physics, 33(4), 1482-1498.

Brajanovski, M., Gurevich, B. and Schoenberg, M. (2005). A model for P-wave attenuation and dispersion in a porous medium permeated by aligned fractures, Geophysical Journal International, 163(1), 372-384.

Chapman, S., Quintal, B. and Tisato, N. (2017). Frequency scaling of seismic attenuation in rocks saturated with two fluid phases, Geophysical Journal International, 208(1), 221-225.

Chen, X. H., Zhong, W. L. and He, Z. H. (2016). Frequency-dependent attenuation of compressional wave and seismic effects in porous reservoirs saturated with multi-phase fluids, Journal of Petroleum Science and Engineering, 147, 371-380.

Dutta, N. C. and Odé, H. (1979a). Attenuation and dispersion of compressional waves in fluid-filled porous rocks with partial gas saturation (White model)-Part I: Biot theory, Geophysics, 44(11), 1777-1788.

Dutta, N. C. and Odé, H. (1979b). Attenuation and dispersion of compressional waves in fluid-filled porous rocks with partial gas saturation (White model)-Part II: Results, Geophysics, 44(11), 1789-1805.

Dvorkin, J. and Nur, A. (1993). Dynamic poroelasticity: A unified model with the squirt and the Biot mechanisms, Geophysics, 58(4), 524-533.

Gelinsky, S., Shapiro, S. A. and Müller, T. M. (1998). Dynamic poroelasticity of thinly layered structures, International Journal of Solids & Structures, 35(34-35), 4739-4751.

Gurevich, B., Zyrianov, V. B. and Lopatnikov, S. L. (1997). Seismic attenuation in finely layered porous rocks: Effects of fluid flow and scattering, Geophysics, 62(1), 319-324.

Krzikalla, F. and Müller, T. M. (2011). Anisotropic P-SV-wave dispersion and attenuation due to inter-layer flow in thinly layered porous rocks, Geophysics, 76(3), WA135-WA145.

Mavko, G. M. and Nur, A. (1975). Melt squirt in the asthenosphere, Journal of Geophysical Research Atmospheres, 80(11), 1444-1448.

Mavko, G. M. and Nur, A. (1979). Wave attenuation in partially saturated rocks, Geophysics, 44(2), 161-178.

Müller, T. M., Gurevich, B. and Lebedev, M. (2010). Seismic wave attenuation and dispersion resulting from wave-induced flow in porous rocks-A review, Geophysics, 75(5), A147-A164.

Norris, A. N. (1993). Low-frequency dispersion and attenuation in partially saturated rocks, Journal of the Acoustical Society of America, 94(1), 359-370.

Pride, S. R., Berryman, J. G. and Harris, J. M. (2004). Seismic attenuation due to wave-induced flow, Journal of Geophysical Research Atmospheres, 109(B1), 59-70.

Rayleigh, L. (1917). On the pressure developed in a liquid during the collapse of a spherical cavity, Philosophical Magazine, 34(200), 94-98.

Song, Y. J., Hu, H. S. and Rudnicki, J. W. (2016). Shear properties of heterogeneous fluid-filled porous media with spherical inclusions, International Journal of Solids and Structures, 83, 154-168.

Sun, W. T., Ba, J. and Müller, T. M. (2015). Comparison of P-wave attenuation models of wave-induced flow, Geophysical Prospecting, 63(2), 378-390.

Sun, W. T., Ba, J. and Carcione, J. M. (2016). Theory of wave propagation in partially saturated double-porosity rocks: a triple-layer patchy model, Geophysical Journal International, 205(1), 22-37.

Wang, Y., Chen, S. and Wang, L. (2013). Modeling and analysis of seismic wave dispersion based on the rock physics model, Journal of Geophysics and Engineering, 10(5), 054001.

White, J. E. (1975). Computed seismic speeds and attenuation in rocks with partial gas saturation, Geophysics, 40(2): 224-232.

White, J. E., Mihailova, N. G. and Lyakhovitskiy, F. M. (1975). Low-frequency seismic waves in fluid-saturated layered rocks, Physics of the Solid Earth, 11, 654-659.

Zheng, P., Ding, B. Y. and Sun, X. T. (2017). Elastic wave attenuation and dispersion induced by mesoscopic flow in double-porosity rocks, International Journal of Rock Mechanics & Mining Sciences, 91, 104-111.

*CORRESPONDING AUTHOR: Zhaoyun ZONG
China University of Petroleum, Qingdao, Shandong, China
email: zhaoyunzong@yahoo.com